CHAPTER II
BACKGROUND AND LITERATURE REVIEW

2.1 Hydroxylation of Phenol

Phenol (PhOH) is one of the pollutants that releases from industrial wastewaters, such as petrochemicals, coal gasification, pesticides manufacture, electroplating and metallurgical operations. It can be found as dilute contaminants in ground waste as well as in surface water. Phenolic derivatives are harmful to aquatic life and have the ability to impart tastes and odors to drinking water even at parts per billion levels. It is in UESEPA list with limits of discharge less than 0.5 mg/L. Moreover, it is believed to be carcinogenic. Therefore, many researchers attempted to convert this pollutant into less toxic products, namely CAT (ortho-dihydroxybenzene) and HQ (para-dihydroxybenzene) are used for various applications (Mohapatra *et al.*, 2003, Das *et al.*, 2005, Adam *et al.*, 2010, Timofeeva *et al.*, 2011, Kumar *et al.*, 2013). CAT can be used as precursor in the production of pesticides, perfumes and pharmaceutical products while HQ is used as a major component in rubber antioxidants, herbicides, and dyestuffs (Adam *et al.*, 2013). Oxidation of phenol is the way to convert phenol into benzenediol. Hydrogen peroxide is often used for the oxidation of phenol, due to its cleanness and less environmental pollutant (by products are water and molecular oxygen)(Abbo *et al.*, 2012).
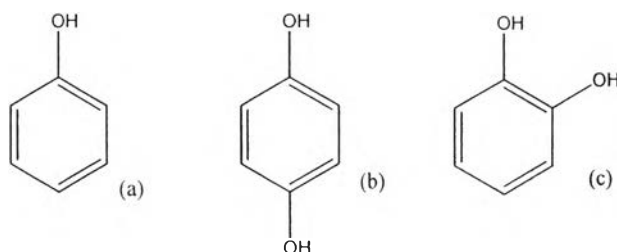

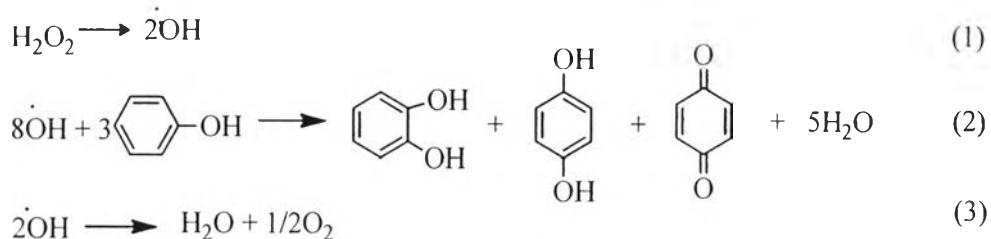**Figure 2.1** Chemical structures of: a) phenol, b) CAT, and c) HQ.

$$H_2O_2 \longrightarrow 2\dot{O}H \tag{1}$$

$$8\dot{O}H + 3 \text{C}_6\text{H}_5\text{OH} \longrightarrow \text{(catechol)} + \text{(hydroquinone)} + \text{(quinone)} + 5H_2O \tag{2}$$

$$2\dot{O}H \longrightarrow H_2O + 1/2 O_2 \tag{3}$$

Figure 2.2 Radical mechanism of hydroxylation of phenol by H_2O_2 (Wu et al., 2008).

Many researchers attempted to oxidize phenol by using H_2O_2 with a variety of homogeneous and heterogeneous catalysts. Homogeneous catalysts are difficult to recover from the reaction mixture and the para-to-ortho ratio is very low (Mohapatra *et al.*, 2003). Therefore, heterogeneous catalysts have been the subject of interest for hydroxylation of phenol due to their properties and catalyst reusability advantages.

Hydroxylation of phenols in the presence of solids containing acid sites occurs by an electrophilic aromatic substitution mechanism at the ortho- or para- positions, as shown in Figure 2.3, activated by resonance of the OH-group of phenol. The formation of CAT and HQ depends on the strength and type of acid if strong acid sites exist in the solid; CAT and HQ are instantaneous formed. However, if their acidity is low, both products will be reduced. However, the complexity of the process goes further, since strong Brönsted sites have also been known to catalyze the decomposition of H_2O_2 that is important competitive reaction of this process (Letaïef *et al.*, 2003).
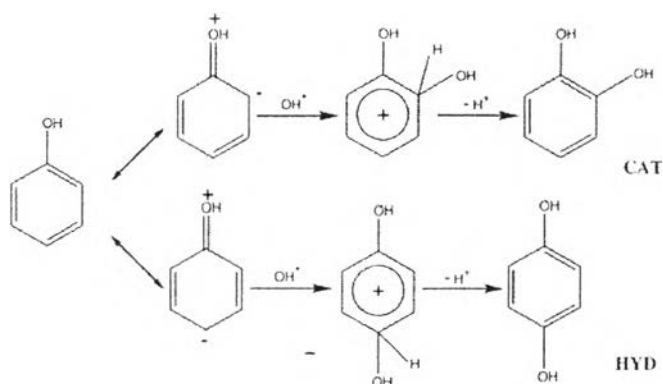
Figure 2.3 The formation of CAT and HQ via electrophilic aromatic substitution mechanism (Letaïef *et al.*, 2003).

Moreover, CAT and HQ also are important intermediates to form various carboxylic acid products, as shown in Figure 2.4.
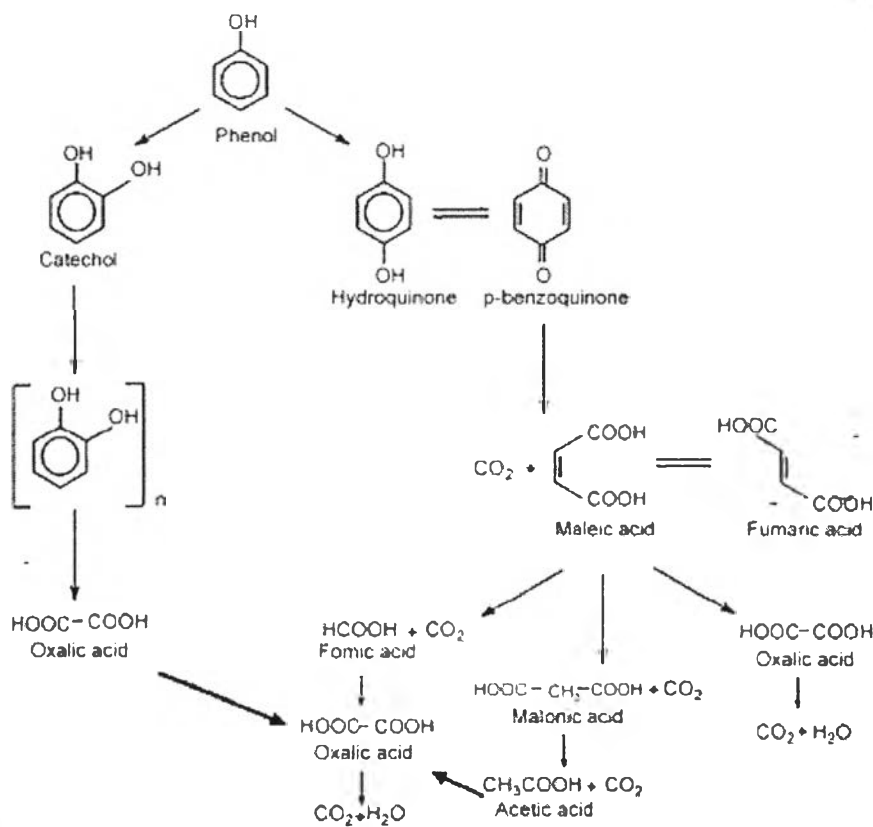

Figure 2.4 Reaction pathway for the phenol electro-catalytic oxidation on mixed metal oxides (Makgae *et al.*, 2008).

2.2 Hydroxylation of Phenol Using Titanium Containing Materials

Titanium dioxide or titania (TiO_2) has been used as catalyst because it can complete photo-oxidation of phenols to mild products, such as water, carbon dioxide, and simple mineral acids (Das *et al.*, 2005). Ti-substituted molecular sieves (Ti^{4+}), such as TS-1, Ti-beta, and Ti-MCM-41, have displayed excellent catalytic properties in selective oxidation reactions when using aqueous hydrogen peroxide as the oxidant (Tanglumlert *et al.*, 2008). Deposition of TiO_2 onto a large internal surface or incorporation of Ti species into the frameworks could exhibit properties that are not found in the single oxide alone (Sahu *et al.*, 2009).

2.2.1 Titanium Silicate-1 (TS-1)

TS-1, one of the highly efficient heterogeneous catalysts, was classified in microporous molecular sieve-based titanosilicate that proved to be excellent catalyst for oxidation of phenol and was commercialized by EniChem Anic S.p.A., Italy. TS-1 was synthesized from alkali-free tetrapropylammonium hydroxide (TPAOH) as template, tetraethyl orthosilicalite (TEOS) as silicon source, and tetrabutylorthotitanate (TBOT) as titanium source. Their active sites were the isolated Ti atoms in the silica matrix (Mohapatra *et al.*, 2003, Liu *et al.*, 2005, Debecker *et al.*, 2013).

Many attempts to use amorphous SiO_2 as a silica source instead of TEOS resulted in the product having properties similar to that synthesized from TEOS (Figure 2.5). Moreover, adding the nonionic surfactant or high ratio of TiO_2/SiO_2 increases the amount of Ti^{4+} incorporated in the framework of zeolite and reduces the amount of TiO_2 in the extraframework, resulting in better catalytic performance of TS-1 for the hydroxylation of phenol (Liu *et al.*, 2005).

Although, TS-1 had a great performance in hydroxylation of phenol, but there were some limitations due to complicated preparation method and their microporous structure that restricted in the oxidation of large molecules (Adam *et al.*, 2010, Debecker *et al.*, 2013). To overcome these limitations, several scientists attempted to discover a cheaper and better catalyst capable of converting this toxic compound into less toxic or useful products. For example, Ti-containing mesoporous

materials, such as Ti-MCM-41 and Ti-MCM-48, are able to catalyze the epoxidation of larger molecules with H_2O_2. Although, heterogeneous catalysts are more active than TS-1 for hydroxylation of phenol, most of them suffer from leaching of the active metal in the liquid phase and behave as homogeneous rather than heterogeneous catalysts (Abbo *et al.*, 2012).
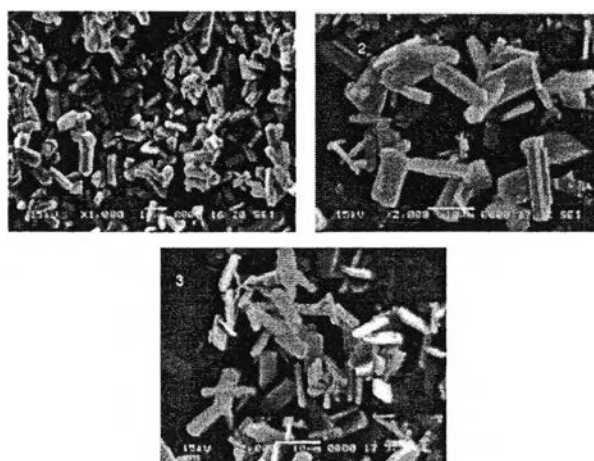

Figure 2.5 SEM micrographs of TS-1 synthesized with amorphous SiO_2 (1), colloidal silica (2), and TEOS (3) (Liu et al., 2005).

2.2.2 Hydroxylation of Phenol Using Titanium on Mesoporous Materials

Since mesoporous materials were first reported in 1992, they had been extensively studied because of their outstanding geometrical properties. These materials were synthesized based on an assembly mechanism between organic surfactants and inorganic precursors, and exhibited a very large surface area (>800 m^2/g), a high porous volume (>1 cm^3/g), a monodisperse pore size (from 2 nm to more than 10 nm), and a regular porous arrangement (Song *et al.*, 2011).

Song and his coworkers synthesized the metallo silicates materials (M-MSU, M = Al, Ti, Zr, etc.) under neutral or near-neutral pH conditions. Nonionic surfactants used can be recovered from the pore channels by nondestructive solvent extraction methods. The pores of MSU were totally nonsymmetric, being constructed from three-dimensional arrays of randomly interconnecting long "worm-like" that decreased the pore blockage and increased the number of reactive surface defect site.

In order to incorporate Ti atoms into the silica framework effectively, modification of the prehydrolysis rate of TEOS played an important role in controlling the incorporation of Ti into the MSU framework. Its catalytic performance on phenol hydroxylation was close to that of TS-1 whereas its preparation cost is much lower (Song *et al.*, 2011).

Table 2.1 Catalytic performance of different samples (Song *et al.*, 2011)

Catalytic performance of different samples.[a]

Catalyst	Phenol conversion (%)	Product selectivity (%)			
		CAT[b]	HQ[c]	Others	CAT/HQ
TS-1[d]	22.5	44.2	53.6	2.2	0.83:1
Ti-MCM-41[e]	15.2	49.9	47.5	2.6	1.05:1
Ti-HMS[f]	9.1	50.1	46.8	3.1	1.07:1
Ti-MSU-6h	19.6	49.0	48.9	2.1	1.03:1

[a]Reaction conditions: water as a solvent, reaction temperature at 60 $^{\circ}$C, phenol/H$_2$O$_2$ = 3/1 (molar ratio), reaction time for 4 h, catalyst/phenol = 10% (weight ratio),

[b]CAT = catechol.

[c]HQ = hydroquinone.

[d]TS-1 with Si/Ti ratio of 100 was synthesized according to a published procedure [26].

[e]Ti-MCM-41 with Si/Ti ratio of 100 was synthesized according to a published procedure [27].

[f]Ti-HMS with Si/Ti ratio of 100 was synthesized according to a published procedure [28].

According to Table 2.1, the conversions in phenol hydroxylation over mesoporous titanosilicates of Ti-MCM-41, Ti-HMS, and Ti-MSU were lower than that over TS-1 due to the relatively low oxidation ability of titanium species in the amorphous nature of the mesoporous wall (Song *et al.*, 2011, Kumar *et al.*, 2013). However, Ti-MCM-68 showed superior activity to TS-1 but a decrease in product yield after some duration of the reaction due to a tar formation was noted (Kumar *et al.*, 2013).
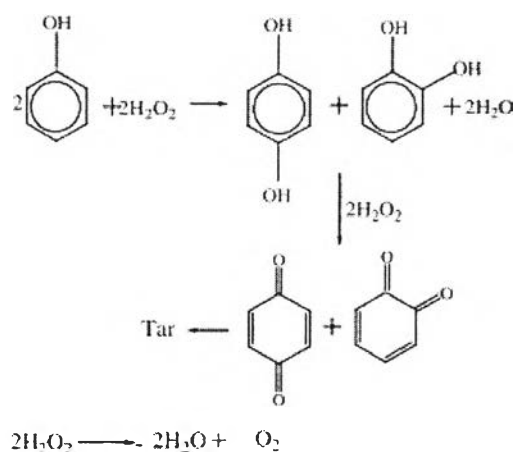
9

$$2H_2O_2 \longrightarrow 2H_2O + O_2$$

Figure 2.6 Schematic diagram of hydroxylation of phenol with H_2O_2 and tar formation (Liu et al., 2008).

Ti-HMA, behaved as heterogeneous catalyst, was a good catalyst for the oxidation of phenol and substituted phenols. It not only showed an outstanding para/ortho ratio of 1.7 for the phenol oxidation reaction at room temperature, but also exhibited high conversion and selectivity for 2, 6-DTBP oxidation. In addition, Ti-HMA could be used to oxidize large organic molecules with good activity (Mohapatra et al., 2003).
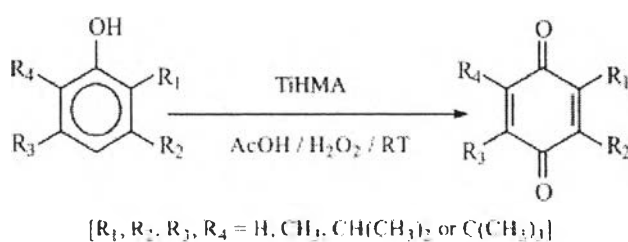

$[R_1, R_2, R_3, R_4 = H, CH_3, CH(CH_3)_2 \text{ or } C(CH_3)_3]$

Figure 2.7 The oxidation of substituted phenols using Ti-HMA at room temperature (Mohapatra et al., 2003).

Several researchers attempted to use SBA-type since their remarkable and 3D-mesopore structure. Ti-SBA-12 had a hexagonal mesopore structure while Ti-SBA-16 had a cage-like cubic interconnected pore structure. Since, the porosity of

Ti-SBA-12 was larger than Ti-SBA-16, thus giving a possible reason for higher activity of SBA-12. Kumar and his coworkers studied the hydroxylation of phenol by using Ti-SBA-12 and Ti-SBA-16 as catalysts. When compared to micropore TS-1, it was found that both Ti-SBA-12 and Ti-SBA-16 were highly active, but their intrinsic catalytic activity was lower than that of TS-1. The intrinsic activity of titanium sites decreases when increasing pore diameter. However, they were more active than Ti-MCM-41 and Ti-SBA-15 since their 3D pore structure helped reactant and product molecules to diffuse to the active sites. Moreover, isolated framework Ti with tetrahedral geometry and ordered mesoporosity were the unique characteristic for the highly efficient phenol hydroxylation activity, and they were reusable with little loss in activity and product selectivity even after the fifth recycle (Kumar *et al.*, 2013).

2.3 Hydroxylation of Phenol Using Iron Containing Mesoporous Materials

Iron-substituted mesoporous materials (Fe^{3+}) had received much attention because of its redox properties and can be used for activity in alkylation, hydrocarbon oxidation, selective reduction, acylation and oxidation reactions using H_2O_2 or N_2O as oxidant. (Choi et al., 2006, Tanglumlert et al., 2008, Zhang et al., 2008)

Adam and his coworkers synthesized heterogeneous catalyst containing Fe-substituted silica derived from rice husk (RH). They found a cheaper way to extract silica by solvent extraction and combined the metal via a sol–gel process at room temperature. They also studied the catalytic activity on oxidation of phenol (Adam *et al.*, 2010).

A series of iron-silica catalyst with (5–20) wt% Fe^{3+} was prepared and studied their catalytic performance. It was found that the activity increased up to 10wt% Fe^{3+} loading. Further increase in the iron content was found to reduce the phenol conversion rate. Higher Fe^{3+} loading (>10% Fe^{3+}) resulted in smaller pore size and exhibited extraframework Fe^{3+} in the catalyst, leading to catalytic deficiency in phenol oxidation. Phenol oxidation by RH-10Fe gave 95.2% conversion at 343K with selective formation of 61.3% CAT and 38.7% HQ. Reusability study with RH-10Fe resulted in only 16% loss in catalytic activity. However, no leaching of iron was de-

tected. The CAT/HQ ratio was found to be constant during the reaction which suggested a non-free radical catalytic mechanism to be operative (Adam *et al.*, 2010).
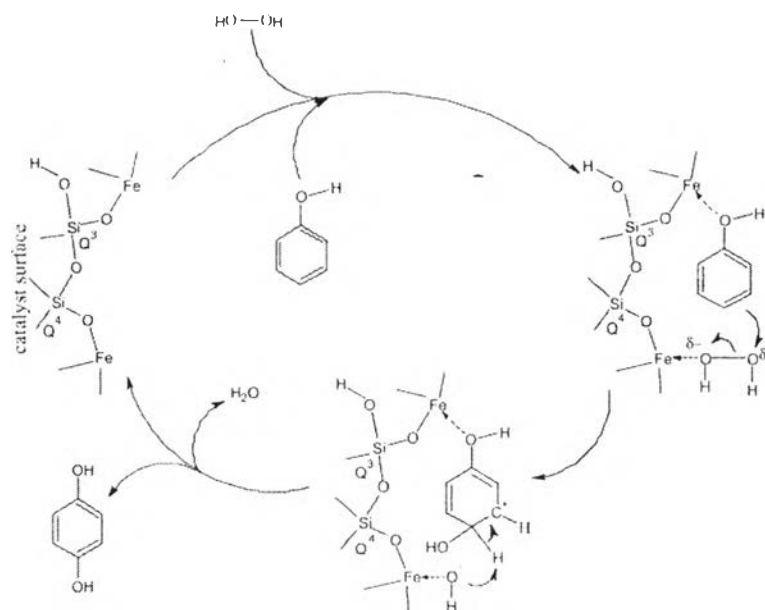

Figure 2.8 The catalytic cycle of the phenol oxidation by H_2O_2 in the presence of RH-10Fe (Adam et al., 2010).

Wu and his coworkers synthesized Fe-MCM41 by using iron nitrate as iron source instead of ferric sulfate and iron trichloride. They found that the catalytic activity increased with iron contents and decreased as Fe/Si molar ratio more than 0.08 (Wu *et al.*, 2007). Meanwhile, Choi and coworkers studied Fe-MCM-41 with 0.5–4 Fe/Si mol%, and found that as the calcination temperature increased from 400 to 800 °C, a higher amount of Fe species came out from the MCM-41 framework. Fe in MCM-41 framework was not stable enough above 750 °C. However, both tetrahedral Fe and extra-framework Fe species were found catalytically active. Fe-MCM-41 was found effective as catalyst in phenol hydroxylation. At 50 °C, phenol conversion of ca. was 60% [when using 1:1 phenol:H_2O_2 and water as solvent]. Surface area, pore volume, and mean pore diameter were 1189 m^2/g, 1.07 c/g, and 36 A°, respectively, with narrow pore size distribution. CAT:HQ ratio in the product was close to 2:1 in accordance with a free radical reaction scheme involving Fe(III)/Fe(II) redox pair.

Higher amount of Fe species always achieved the given phenol conversion at a shorter reaction time, as compared to other Fe-containing catalysts, such as Fe-salt impregnated MCM-41 and Fe_2O_3 nano-particles. Furthermore, Fe-salt impregnated MCM-41 is believed to be made of mostly extra-framework Fe oxides, thus phenol conversion was lower than Fe-MCM-41 with longer reaction time, indicating that octahedral extra-framework Fe species were less active than tetrahedrally coordinated material. Moreover, the conversion of phenol was strongly dependent on the solvent, as shown in Figure 2.9.
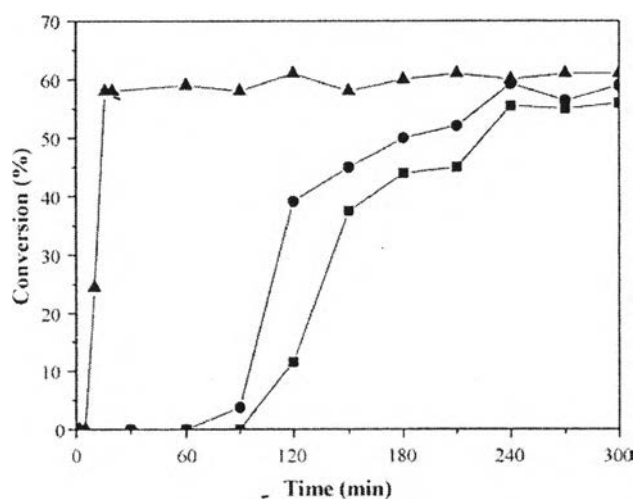

Figure 2.9 Catalyst recycling effect on the phenol conversions at 50 °C using 1:1 phenol:H_2O_2 in water over Fe-MCM-41 calcined at 550 °C; (▲) first cycle (4 mol%), (●) second cycle (2.8 mol%), (■) third cycle (2.5 mol%) (Fe/Si measured by SEM–EDS) (Choi et al., 2006).

Phenol hydroxylation did not work in acetone or in ethanol (less than ca. 4%) because ethanol is scavenger of hydroxyl radical, and slight reaction took place. In water, both phenol and H_2O_2 are dissolved easily and active hydroxyl radicals can be formed when H_2O_2 contacts with Fe sites, as shown in Figure 2.10. This effect of the solvents strongly supports radical reaction mechanism in phenol hydroxylation. Radicals generated are more stable in polar solvents, and the polarity order of the

solvents is water > acetonitrile > acetone and ethanol, which was exactly the same order as the results of phenol conversions obtained in the study.
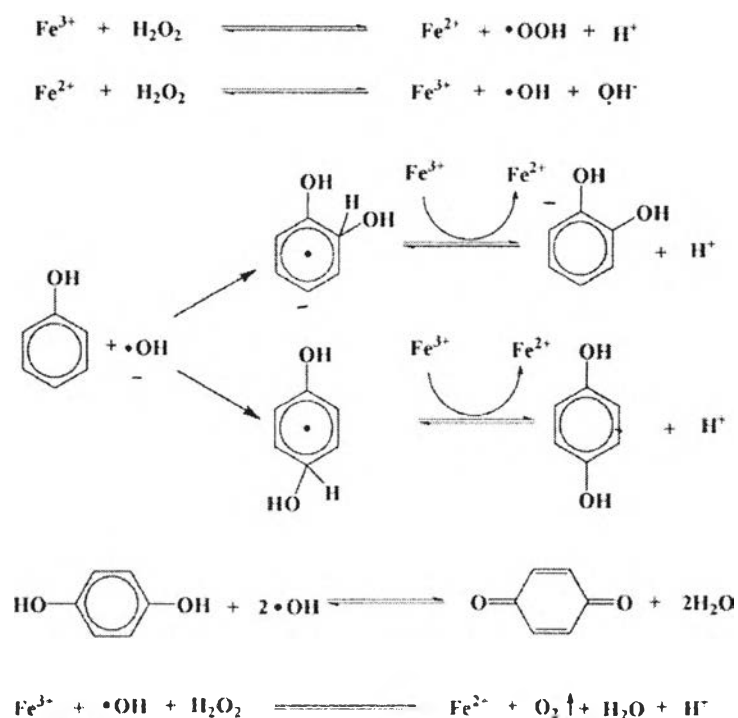

Figure 2.10 Phenol hydroxylation reaction pathway of Fe ions (Choi et al., 2006).

From SEM–EDS analysis, Fe contents of these catalysts decreased from 4 to 2.8 and 2.5%, respectively. It was stable after 2–3 runs. At the first reaction, phenol conversion was higher due to extra-framework Fe clusters contributing to the radical reaction. It was assumed that under acidic condition Fe clusters of extra-framework was partly removed, but framework Fe species remained more or less conserved in the second and third run (Choi *et al.*, 2006).

Fe-containing nickel phosphate molecular sieves (Fe-VSB-5) were hydro-thermally synthesized in weak basic conditions under microwave irradiation. It was found that the increasing of iron content in Fe-VSB-5 led to an increase in the reaction rates since Fe increased the radical generation, as shown in Figure 2.11. The 6.5%Fe-VSB-5 was stable against leaching of iron species and could be used repeat-

edly in an oxidation reaction without suffering a loss of activity (Timofeeva *et al.*, 2011).
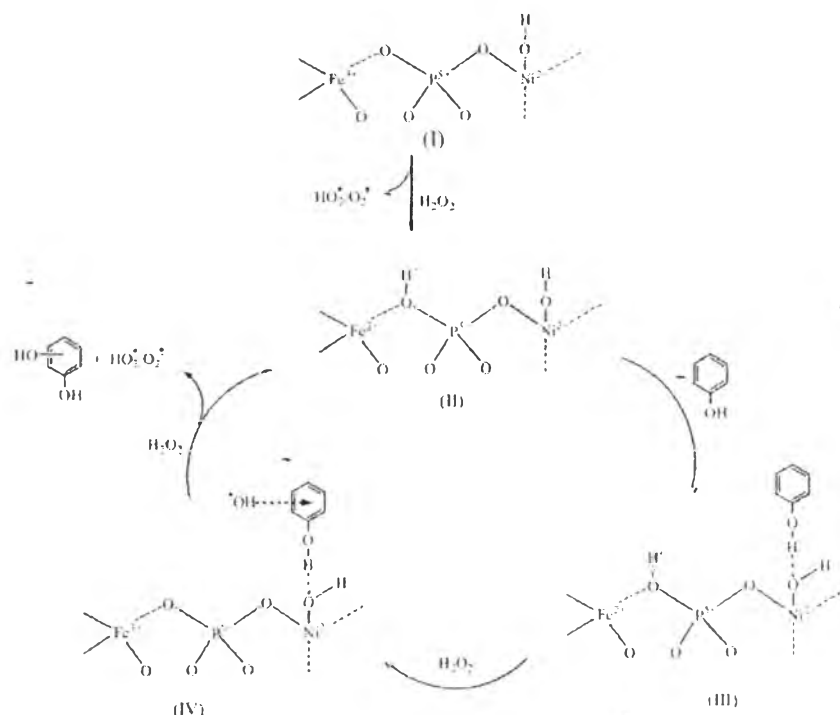
Figure 2.11 Proposed mechanism of phenol oxidation with H_2O_2 over Fe-VSB-5 (Timofeeva et al., 2011).

HMS, one of mesoporous materials, was easily synthesized by the sol–gel process via S^0I^0 assembly pathway, using alkylamine as the structure directing agent, TEOS as a silica source, and $Fe(NO_3)_3 \cdot 9H_2O$ as iron precursor. They have thicker framework walls with wormhole framework structure. Liu and his coworkers attempted to synthesize Fe-HMS for phenol hydroxylation by using various types of surfactants and used isopropanol as co-surfactant. It was found that Fe^{3+} ions incorporated into the HMS framework showed a good catalytic performance for the hydroxylation of phenol. The catalytic activity of Fe_2O_3 in the extraframework of HMS was very low since extra iron oxides accelerated a decomposition of H_2O_2. If Fe/Si >0.03, some polymerized Fe species in the extraframework were appeared, therefore the phenol conversion decreased. The Fe-HMS sample prepared with the synthesis

gel of $DDA/SiO_2 = 0.27$, $H_2O/SiO_2 = 100$, $EtOH/SiO_2 = 9.0$ for 30 h synthesis time had the best performance for the phenol hydroxylation (Liu *et al.*, 2008).

2.4 Hydroxylation of Phenol Using Bimetallic (Fe or Ti) Incorporated Materials

Timofeeva and coworkers attempted to synthesize the Fe-Al-silica mesoporous catalysts for phenol hydroxylation. The Fe-Al-containing mesoporous silicate materials, denoted as Fe-Al-MMM-2, were synthesized under weak acidic conditions (pH 2.4–4.4) using Keggin type cation $[FeAl_{12}O_4(OH)_{24}(H_2O)_{12}]^{7+}$ ($FeAl_{12}^{7+}$) as Al and Fe sources. It was found that pH affected to the properties of Fe-Al-MMM-2 since $FeAl_{12}^{7+}$ cation was not stable at pH 2.3 and 3.3. Furthermore, the increase of Al content decreased catalytic activity in all reactions since, it increased the strength of basic sites of Fe-containing samples, leading to the increase of H_2O_2 degradation rate. Moreover, addition of Al increased the surface acidity due to the changes of type and content of OH-groups which facilitated the sorption–desorption processes of reagents. It was demonstrated that in the hydroxylation of phenol selectivity towards HQ was varied by increasing Al content in the sample. In full phenol oxidation with H_2O_2, Fe-Al-MMM-2 (pH 4.4) was found to be more active, comparing to Fe-Al-PILC (pH 4.4) (Timofeeva *et al.*, 2010).

Zhang and his coworkers attempted to synthesize Ce-Fe-SBA-15 by a pH-adjusted hydrothermal method for studying the mechanism of phenol hydroxylation by H_2O_2. They also found that the mechanism was commonly through a radical mechanism.

2.5 Mesoporous Materials

According to IUPAC classification, porous materials can be categorized into three groups by their pore size. The first group is microporous materials that have pore diameter less than 2 nm, such as zeolite. The second one is mesoporous materials that have pore diameter between 2 nm to 50 nm. The last one is macroporous materials having pore diameter larger than 50 nm.

One advantage of mesoporous materials is their amorphous wall which can be incorporated by various elements or organic groups. Another advantage is their huge inner surface which can be easily modified (Phiriyawirut *et al.*, 2003, Huo, 2011).

Silica is widely employed as main building block of mesoporous materials because it is inexpensive, thermally stable, chemically inert, harmless, and abundantly available in the Earth's crust. One of mesoporous materials synthesized using silica is Santa Barbara Amorphous no 15 (SBA-15), see Figure 2.12 (Norhasyimi, 2010).
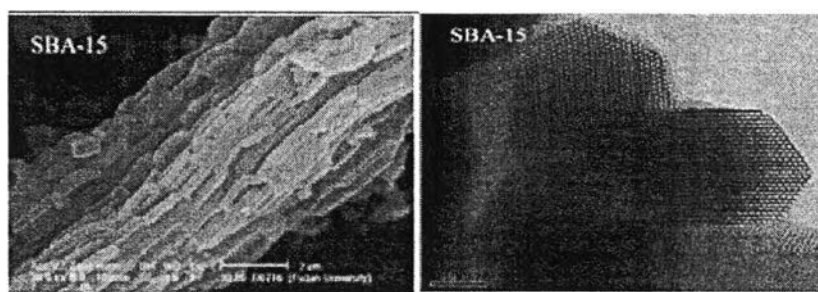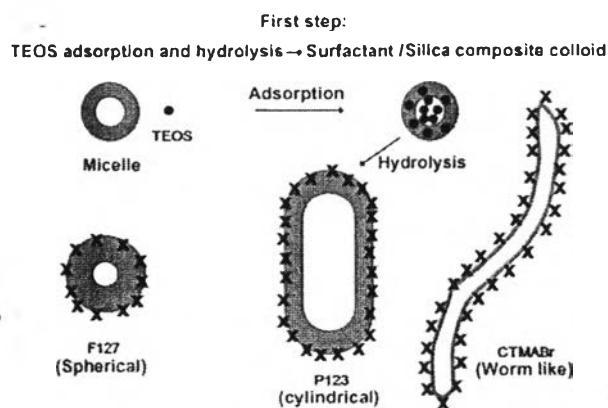

Figure 2.12 a) SEM and b) TEM of SBA-15 (Song et al., 2012).

2.6 Introduction to SBA-15

SBA-15, discovered in 1998, has a 2D uniform hexagonal pores (*P6mm*) with a narrow pore size distribution and a tunable pore diameter of between 5 and 15 nm (or up to 4.6–30 nm) (Norhasyimi, 2010). The thickness of the framework wall is up to 3–7 nm (Taguchi *et al.*, 2005) which gives the material a higher hydrothermal/mechanical stability, chemical resistance properties than MCM-41. Its high internal surface area of 400–900 m^2/g makes SBA-15 a well suited material for various applications. It can be used in environmental analytics for adsorption and separation, advanced optics, as a support material for catalysts, drug delivery media, and as a hard template for the production of nanostructured carbon or platinum replica etc. (Taguchi *et al.*, 2005, Norhasyimi, 2010, Thielemann, 2011, Song *et al.*, 2012).

2.6.1 SBA-15 Synthesis

Basically, SBA-15 was synthesized from tetramethylorthosilicate (TMOS), tetraethylorthosilicate (TEOS) or tetrapropylorthosilicate (TPOS) as silica source. Many scientists have attempted to synthesize SBA-15 using other silica sources, such as low silica inorganic precursor, consisting of metal oxide containing 42 wt%SiO_2 (Norhasyimi R., 2010) and obtained from industrial waste product without pre-purification. This can be cost effective for bulk production while Wongkasemjit's group (Samran *et al.*, 2011) uses home-made silatrane easily synthesized from silica and triethanolamine. Generally, SBA-15 synthesis requires triblock co-polymers surfactant, consisting of poly(ethyleneoxide)$_x$-poly-(propylene oxide)$_y$-poly(ethylene oxide)$_x$, $(PEO)_x(PPO)_y$-$(PEO)_x$, (trade name: Pluronics123, P123) where x=30, y=70, PPO = hydrophobic core, and PEO = hydrophilic chains, acting as structural directing agent to form liquid-crystal structures. Micelles of the surfactant are surrounded by a framework of polycondensed silica, see Figure 2.13 (Mesa *et al.*, 2008). Most researchers obtained SBA-15 under strongly acidic conditions, such as HCl. The increased amount of HCl increases the hydration rate of the silica precursor, which can be used to control the thickness and the length of the rods (Johansson, 2010). Moreover, if pH is higher than the isoelectric point of silica, i.e., at pH 2.0, there are no precipitation or formation of silica gel. Disordered or amorphous silica would likely happen at the neutral pH of 7. However, SBA-15 could also be synthesized by the prehydrolysis of TEOS at pH<3 and interacting with template agent to form a mesophase under weak acidic condition (Norhasyimi 2010).
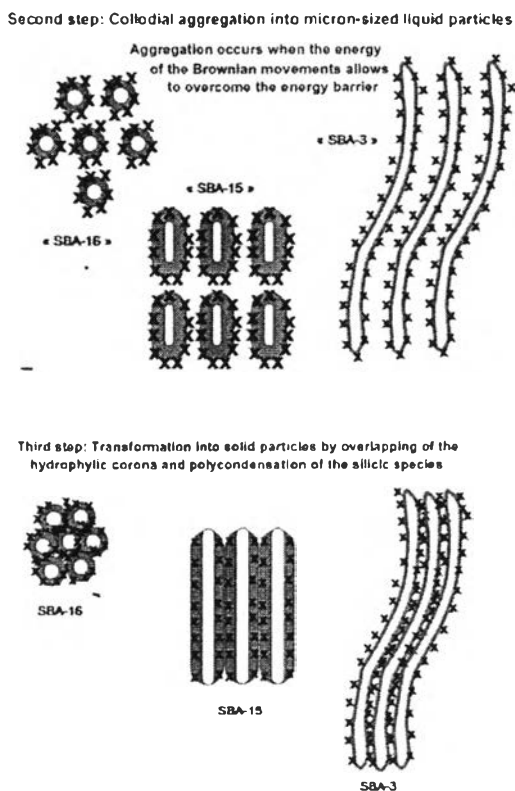

First step:
TEOS adsorption and hydrolysis → Surfactant /Silica composite colloid

Second step: Collodial aggregation into micron-sized liquid particles

Aggregation occurs when the energy
of the Brownian movements allows
to overcome the energy barrier

« SBA-3 »

« SBA-15 »

« SBA-16 »

Third step: Transformation into solid particles by overlapping of the
hydrophylic corona and polycondensation of the silicic species

SBA-16

SBA-15

SBA-3

Figure 2.13 The mechanism of SBA-n formation (Mesa *et al.*, 2008).

After synthesis, the template must be removed, and the template re-
moval was one of the crucial steps since this procedure could modify the final prop-
erties of a desired porous structure (Norhasyimi, 2010). The template can be re-
moved by calcination, washing, reflux extraction, acid, H_2O_2 treatment, extraction
with supercritical CO_2, and microwave digestion. Moreover, there are some re-
searchers attempting to use solvent to remove organic materials, such as water, ace-
tone or ethanol etc. Using ethanol instead of water provides three times more effec-
tive in removing the template from the SBA-15 framework, notwithstanding P123
cannot be removed completely from the SBA-15 by washing (Thielemann, 2011).
Thielemann and coworkers used a combined solvent of water and ethanol and found
that the surface area was increased; however, SBA-15 may change if large amount of
solvent was used.

The outstanding feature of SBA-15 is the **microporosity** which is pre-
sent in its mesopore wall, These microporous structures are generally disordered and

provide interconnectivity between the ordered mesopores (Norhasyimi Rahmat, 2010). From the XRD results, it was found that the walls had a "microporous corona" region, resulting from partial embedding of the PEO part of the surfactant in the silica wall. This corona was converted to micropores upon calcination. The morphology and extent of intrawall microporosity of SBA-15 depended on the synthesis conditions, such as silica source, length of the ethylene oxide blocks, silica/template ratio, aging period/temperature, pH of mixture, and presence of inorganic salt. For example, an increase of aging temperature from 60° to 130 °C decreased the pore volume fraction of micropores from 30 to 5% (Zukerman *et al.*, 2008). The different amounts of micropores, changed in the pore wall thickness, and the morphology of SBA-15 could be obtained by changing the template, post-synthesis treatment, or varying synthesis conditions, like temperature, the addition of additives, such as co-surfactants, swelling agents, electrolytes, salts, etc. There were two types of micropores: originating from the walls and the nanocapsules. The micropore volume was approximately 0.1 cm^3/g or the total pore volume could exceed to 1 cm^3/g (Taguchi *et al.*, 2005, Huo, 2011). The intrawall pores display a wide range of sizes, including "regular" micropores (1–2 nm), ultramicropores (<1 nm) and small mesopores (2–5 nm), providing the opportunity to manipulate the mesoporous materials in preparation of novel materials with potential applications. Firstly, increasing microporosity enhances hydrothermal stability. Micropores in SBA-15 were critical for preparation of ordered nanostructures, like carbon and platinum replicas. The porosity of the walls may also promote molecular transport. Moreover, the adsorption interaction of toluene with SBA-15 was stronger in the micropores than in the mesopores (Zukerman *et al.*, 2008).

Although, SBA-15 has many advantages, pure SBA-15 still has some drawbacks i.e. low acidity strength. To overcome its limitation some researchers attempted to enhance and optimize its catalytic activity by supporting or immobilizing other elements or complement other catalyst, especially for thermal enhance, reusability, and enzymatic activity (Norhasyimi, 2010).

2.6.2 Silatrane Precursor

Wongkasemjit's group has used home-made silatrane as the silica source for synthesis of both micro- and mesoporous materials because it is moisture

resistance, resulting in slower hydrolysis rate. Moreover, it is easy to handle and control (Phiriyawirut *et al.*, 2005, Samran *et al.*, 2011). Oxide-one-pot-synthesis of silatrane is carried out under nitrogen atmosphere with continuous removal of water generated as by-product from the condensation reaction. The silatrane product is purified by washing with acetonitile to remove excess TEA and EG. Silatrane is more resistive to hydrolysis than other types of silicon alkoxide. Scheme 2.1 showed all chemical reagents needed for the silatrane synthesis.
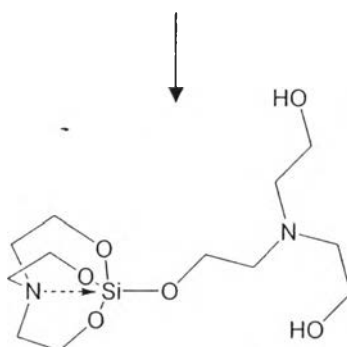
$$SiO_2 + N(CH_2CHCH_3OH)_3 + H_2NCH_2(CH_2NHCH_2)_2CH_2NH_2 + HOCH_2CH_2OH$$

Figure 2.14 Preparation of silatrane precursor (Samran *et al.*, 2011).

Characterization by FTIR is shown in Table 2.1. From XRD result (Figure 2.15) confirmed that silatrane is a crystalline product.

Samran *et al.* in 2011 successfully synthesized SBA-15 at room temperature using silatrane. The crystallographic, morphological, and physical properties of the SBA-15 obtained by this simple process were comparable to mesoporous silica prepared by a more complicated microwave-assisted hydrothermal method. This simple and room temperature preparation method provides inexpensive, energy-saving, and efficient production of SBA-15 for a range of catalytic and environmental applications. Moreover, they also successfully synthesized Fe-, or Ti-SBA-15 using silatrane for styrene epoxidation (Samran *et al.*, 2011).

Table 2.2 FTIR Peak positions and assignments of the synthesized silatrane (Phiriyawirut *et al.*, 2003)

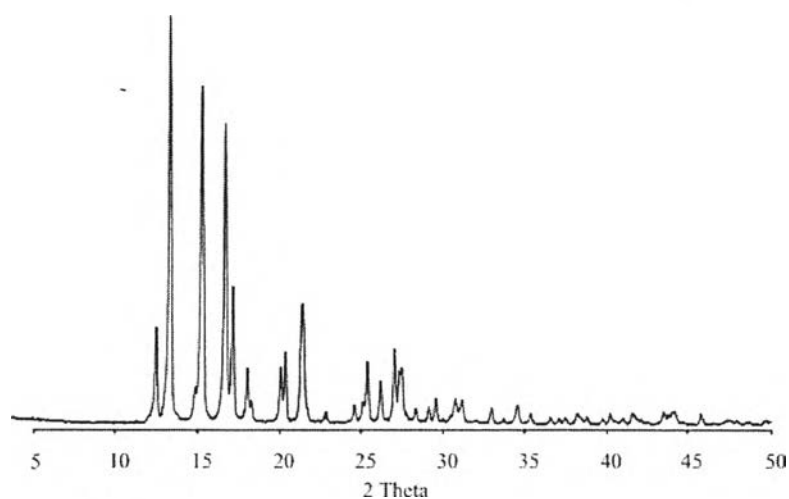| Peak positions (cm^{-1})	Assignments
3100–3700	b, ν(O–H)
2800–3000	s, ν(C–H)
2750–2670	w, NR$_3$ salt (Si←N)
1445, 1459, 1493	m, δ(C–H)
1351	w, ν(C–N)
1276	m, ν(C–O)
1040–1180	b and vs, ν(Si–O)
786	vs, δ(Si–O–C)
735	s, δ(Si–O–C)
576	w, Si←N

Figure 2.15 XRD pattern of silatrane (Phiriyawirut et al., 2003).

2.6.3 Bimetallic Incorporated on SBA-15

2.6.3.1 Ce-Fe Incorporated on SBA-15

Zhang and his coworkers synthesized Ce-Fe-SBA-15 using a pH-adjusted hydrothermal method by directly adding the $(NH_4)_2Ce(NO_3)_6$ and $Fe(NO_3)_3$ as cerium and iron sources, respectively. They found that when the solution was at pH 2.3 which is higher than the isoelectric point of SiO_2 (at pH 2.0), the Si species showed negative charge and the same charges as Ce in the solution, indicat-

ing the difficulty of the interaction between Ce and Si species. Thus, the dehydrox-ylation effect of M–OH and Si–OH to form M–O–Si bond in hydrothermal condition was another reason for the high contents of Fe and Ce in the final products which was more important than electrostatic force. Moreover, all the samples displayed typical hexagonal arrangement of mesoporous structure with high surface area. They believed that Fe promoted the incorporation/dispersion behavior of Ce into the SBA-15. Furthermore, addition of Fe made pore parameters increase, such as pore volume: from 0.74 to 1.3, a_0: from11.2 to 13.0, etc. The increase of a_0 and pore diameter values could be taken as an indication of the incorporation of the metals in the silica framework. Meanwhile, an increase in the Ce content in Ce(x)–Fe(3.5)-SBA-15 samples made the pore volume decrease from 1.28 to 0.88 (Zhang *et al.*, 2008).

2.6.3.2 Fe-Mo Incorporated on SBA-15

Zhang and coworkers studied bimetallic Fe-Mo-SBA-15 via sol-gel synthesis by direct adding TEOS, $(NH_4)_6Mo_7O_{24}$, and ferric nitrate as silica, molybdenum, and iron sources, respectively. pH was adjusted by HCl to pH 2.3. They found that addition of molybdic species enhanced the structural ordering of mesoporous materials. However, Mo species did not incorporate into the framework. It only dispersed on the pore of SBA-15. From XRD pattern, when increasing the iron contents, d_{100} changed, confirming the incorporation of iron species. DR-UV spectroscopy at below 300 nm exhibited Fe^{3+} or Mo^{6+} in tetrahedral geometry. There was shoulder around 343 nm which described the M-O-M species. Around 515 nm was detected, indicating the presence of Fe_2O_3 or MoO_3. Furthermore, Molybdenum decreased the reducibility of Fe species and increased the reduction temperature as well. It promoted the intensity of surface acidity and amount of surface acid sites when compared to Fe-SBA-15 (Zhang *et al.*, 2012).

2.6.3.3 Co-Fe Incorporated on SBA-15 and HMS

Bragançe and coworkers tried to synthesize monometallic and bimetallic Co and/or Fe deposited on HMS and SBA-15 by impregnation for Fischer-Tropsch synthesis. Co and Fe sources were derived from $Co(NO_3)_2 6H_2O$ and $Fe(NO_3)_3 9H_2O$, respectively. From XRD patterns in Figure 2.16, they displayed typical diffraction peak (d_{100}) after calcination. It confirmed that the mesoporous supports maintained ordered structure after metal impregnation and calcination steps.
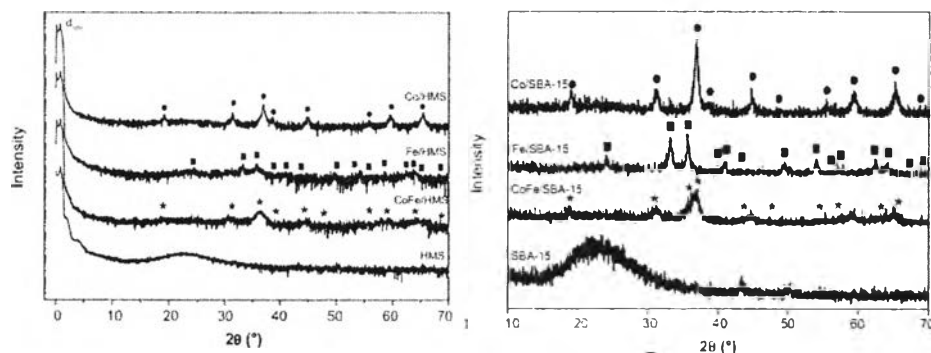
Figure 2.16 X-rays diffraction patterns recorded for the HMS (left) and SBA-15 (right) support and mono/bimetallic Co/Fe clusters deposited on HMS. Phase identification: (●) Co_3O_4 ; (■) Fe_2O_3 ; (*) $CoFe_2O_4$.

Table 2.2 summarized the results of the Co/Fe ratio from AAS. It was lower than that indicated in XRD, suggesting the presence of an amorphous Fe phase undetectable by XRD. However, their performances in catalytic tests of the bimetallic catalysts were closer to the iron catalysts (Bragançe *et al.*, 2012).

Table 2.3 Metal loading (wt%) of the calcined mono/bimetallic Co-Fe catalysts (Bragançe *et al.*, 2012)

Catalyst	AAS[a]			XRD[b]		
	Co	Fe	Co/Fe at. ratio	Co	Fe	Co/Fe at. ratio
Co/HMS	23	-	-		-	-
Fe/HMS	-	24	-	-		-
Co-Fe/HMS	14	10	1.4			2
Co/SBA-15	24	-	-	-		-
Fe/SBA-15	-	24	-	-		-
Co-Fe/SBA-15	15	13	1.2			23

[a] Atomic absorption spectroscopy (AAS), [b] X-ray diffraction (XRD)

$$H_2O_2 \longrightarrow 2 \cdot OH \qquad (1)$$

$$2 \cdot OH + \text{[phenol]} \longrightarrow \text{[catechol]} + \text{[hydroquinone]} + \text{[benzoquinone]} \qquad (2)$$

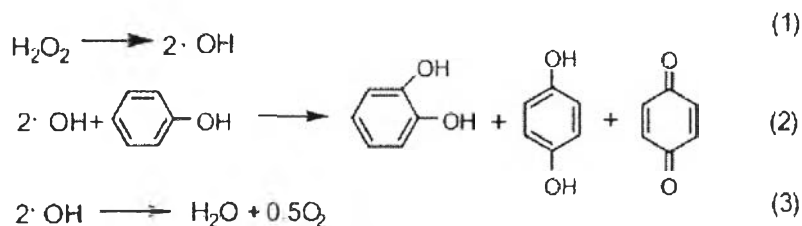$$2 \cdot OH \longrightarrow H_2O + 0.5 O_2 \qquad (3)$$

Figure 2.17 Proposed common reaction mechanism for the formation of diphenol in phenol hydroxylation (Zhang et al., 2008).

There were two competitive reactions for OH⁻ between de--composed (step3) and reacted with phenol (step 2). High concentration of OH⁻ preferred step 3. On the other hand, low concentration of OH⁻ followed to step 2. The concentration of OH⁻ was determined by step 1, which was catalyzed by Fe in Ce–Fe-SBA-15. Increasing amount of Ce in Ce(x)–Fe(3.5)-SBA-15 samples, The pore volume decreased from 1.28 to 0.88. It could be indicated that Ce in Ce(x)–Fe(ca. 3.5)-SBA-15 samples may be mostly dispersed on the wall surface. In contrast, when Fe content increased in Ce(ca. 1.8)–Fe(y)-SBA-15 samples, the changes of pore parameters (V_p: from 0.74 to 1.3, a_0: from 11.2 to 13.0, etc.) were obvious. The increasing of a_0 and d_p was the result of incorporation of the metals in the silica framework.

$$Ce^{4+} \overset{NO_3^-}{\rightleftharpoons} [Ce(NO_3)]^{3+} \overset{NO_3^-}{\rightleftharpoons} [Ce(NO_3)_2]^{2+} \overset{NO_3^-}{\rightleftharpoons} [Ce(NO_3)_6]^{2-} \qquad (1)$$

$$Fe(OH)^{2+} \rightleftharpoons [Fe_2(OH)_2]^{4+} \qquad (2)$$

$$\text{Ce species + Fe species} \overset{\text{electrostatic affinity}}{\rightleftharpoons} \text{Ce-Fe species (-OH containing)} \qquad (3)$$
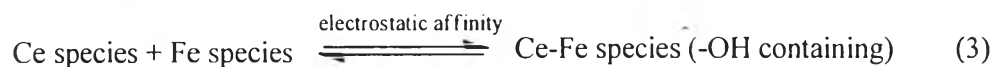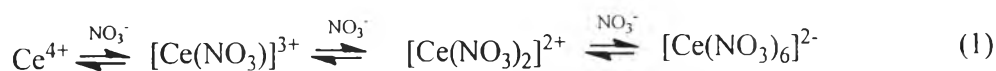
Figure 2.18 The possible mechanisms that can occurred at various pH (Zhang et al., 2008).

Moreover, the pH was affected to mechanism of reaction that shown in Figure 2.18, it was found that when pH of mixture is 2.3 that is higher than isoelectric point of Si (pH 2.0) therefore, Si will become negative charge caused in-

teraction between Ce and Si is more difficult. It was believed that it related to the de-hydroxylation effect of M–OH and Si–OH to form M–O–Si bond in hydrothermal circumstance is another reason for the high contents of Fe and Ce in the final products. $[Fe_2(OH)_2]^{4+}$ was formed first, Then this mixed species could react with the Si species. When Ce species or Fe species were at a low concentration in the solution, the Eq. (3) tended to shift to the left, which led the low utility of the Ce species. As the concentration of Ce species and Fe^{3+} increased at the starting solution, all these three equations shifted to the right hand side, which led to the easier co-condensation of cerium and iron species thus amount of Si species and Ce in final product were raised. Ce species played two roles. Firstly, used as promoter in redox reactions, the introduction of Ceria could efficiently improve the diphenol distribution. Secondly, although Ce was commonly not considered as a good catalyst in phenol hydroxylation, but the HQ in the final product was raised. It suggested that samples with an appropriate Ce/Fe ratio would be the optimal catalyst for the reaction.